Human Molecular Genetics, 2012, Vol. 21, No. 13 **3001–3012**
doi:10.1093/hmg/dds130
Advance Access published on April 5, 2012

Ube3a-ATS is an atypical RNA polymerase II transcript that represses the paternal expression of *Ube3a*

Linyan Meng, Richard E. Person and Arthur L. Beaudet*

Department of Molecular and Human Genetics, Baylor College of Medicine, Houston, TX 77030, USA

Received March 12, 2012; Revised March 12, 2012; Accepted April 2, 2012

The Angelman syndrome gene, *UBE3A*, is subject to genomic imprinting controlled by mechanisms that are only partially understood. Its antisense transcript, *UBE3A-ATS*, is also imprinted and hypothesized to suppress *UBE3A in cis*. In this research, we showed that the mouse antisense ortholog, *Ube3a-ATS*, was transcribed by RNA polymerase (RNAP) II. However, unlike typical protein-coding transcripts, *Ube3a-ATS* was not poly-adenylated and was localized exclusively in the nucleus. It was relatively unstable with a half-life of 4 h, shorter than most protein-coding RNAs tested. To understand the role of *Ube3a-ATS in vivo*, a mouse model with a 0.9-kb genomic deletion over the paternal *Snrpn* major promoter was studied. The mice showed partial activation of paternal *Ube3a*, with decreased expression of *Ube3a-ATS* but not any imprinting defects in the Prader–Willi syndrome/Angelman syndrome region. A novel cell culture model was also generated with a transcriptional termination cassette inserted downstream of *Ube3a* on the paternal chromosome to reduce *Ube3a-ATS* transcription. In neuronally differentiated embryonic stem (ES) cells, paternal *Ube3a* was found to be expressed at a high level, comparable with that of the maternal allele. To further characterize the antisense RNA, a strand-specific microarray was performed. *Ube3a-ATS* was detectable across the entire locus of *Ube3a* and extended beyond the transcriptional start site of *Ube3a*. In summary, we conclude that *Ube3a-ATS* is an atypical RNAPII transcript that represses *Ube3a* on the paternal chromosome. These results suggest that the repression of human *UBE3A-ATS* may activate the expression of *UBE3A* from the paternal chromosome, providing a potential therapeutic strategy for patients with Angelman syndrome.

INTRODUCTION

In mammals, a small percentage of genes are imprinted, leading to the differential expression of the paternal and maternal alleles. These genes are usually located in clusters, spanning several megabases on the chromosome, and regulated by an imprinting center (IC) (1,2). Human chromosome 15q11-q13 is such a region known as the Prader–Willi syndrome (PWS)/Angelman syndrome (AS) region, since its deletion on the paternal chromosome leads to PWS (MIM ID: 176270) and deletion on the maternal chromosome leads to AS (MIM ID: 105830) (3). In this region, paternally expressed genes include *SNRPN-SNURF*, *NDN* and a cluster of snoRNAs. Their silencing on the maternal chromosome is mainly attributed to DNA methylation and histone modifications at the PWS-IC conferred by the AS-IC, which together form a bipartite IC regulating the imprinted status of this region (4,5). *UBE3A*, on the other hand, is maternally expressed in neurons. *UBE3A* encodes an E3 ubiquitin ligase named E6-AP and is known to be the major disease gene for AS, which is a neuro-developmental disorder characterized by severe developmental delay, speech impairment, a movement disorder, seizures and inappropriate happy disposition (6–8). However, the imprinting mechanism of *UBE3A* appears to be different from those paternal genes in that (i) it is biallelically expressed in most cell types but imprinted in neurons (9–12); and (ii) its promoter is not associated with differential DNA methylation on the silent paternal chromosome versus the active maternal chromosome (13–15). Since the genomic structure and the imprinting pattern are highly conserved in *Mus musculus*, mouse models are extremely useful in studying the imprinting mechanism of this region.

*To whom correspondence should be addressed at: Department of Molecular and Human Genetics, Baylor College of Medicine, One Baylor Plaza, MS BCM225, Houston, TX 77030, USA. Tel: +1-7137984795; Fax: +1-7137987773; Email: abeaudet@bcm.edu

Epigenetic silencing in association with antisense RNAs has been observed in many cases including *Xist/Tsix*, *Igf2r/Airn* and *Kcnq1/Kcnq1ot1* (16–18). The latter two are of particular interest because both are involved in genomic imprinting. Silencing of *Igf2r* and *Kcnq1* on the paternal chromosome is associated with the *cis* expression of the antisense RNAs, *Airn* and *Kcnq1ot1*, respectively. Mice carrying a transcriptional stop mutation in the *Airn* or *Kcnq1ot1* antisense transcripts show the complete unsilencing of the imprinted genes in the cluster, including the overlapping transcript, *Igf2r* or *Kcnq1*, respectively (19,20). These mouse models suggest a necessity of these antisense RNAs in establishing the imprinting status of the overlapping sense transcript. The two antisense RNAs share additional features. The transcription of both is regulated by DNA methylation at the IC as both promoters are embedded in a differentially methylated region (DMR). *Kcnq1ot1* and the majority of *Airn* also escape RNA splicing and nuclear export, distinguishing them from typical RNA polymerase (RNAP) II transcripts (21,22).

The antisense transcript of *UBE3A* (*UBE3A-ATS*) was first identified in human in 1998 (23). In both human and mice, the antisense RNA (*UBE3A-ATS* or *Ube3a-ATS*) is part of a large transcript that initiates at and upstream of the PWS-IC (24,25). In mice, this large transcript is named *LNCAT* for *large non-coding antisense transcript* and extends over ~1000 kb through *Snrpn-Snurf*, snoRNAs, *Ipw* and *Ube3a* (25,26). The antisense RNA is specifically expressed from the paternal chromosome in neurons, where *Ube3a* imprinting occurs (11). Deletion of the PWS-IC in mice represses the expression of *Ube3a-ATS* and activates the normally silenced paternal *Ube3a* (27). On the contrary, when the mouse IC is replaced with the human ortholog, the maternal chromosome acquires a paternal expression pattern with activation of *Snrpn*, snoRNAs, *Ube3a-ATS* and silencing of *Ube3a* (28). All the evidence is consistent with the hypothesis that *Ube3a-ATS* directly mediates silencing of paternal *Ube3a* (6,29). However, a direct causal relationship between *Ube3a-ATS* and *Ube3a* silencing has not been established.

In the present study, we showed that *Ube3a-ATS* is an atypical RNAPII transcript that functions to suppress paternal *Ube3a* expression. Elimination of the expression/transcription of human *UBE3A-ATS* may provide a novel approach for activating the expression of *UBE3A* from the paternal chromosome as a treatment for Angelman syndrome.

RESULTS

Ube3a-ATS is an atypical RNAPII transcript

Ube3a-ATS is mono-allelically expressed from the paternal chromosome in neurons and has been shown to be part of the large transcript, *LNCAT* (24,25). It is highly heterogeneous as northern blot analysis shows smearing rather than a single or multiple bands (30). Besides these facts, very little is known about this extraordinarily long mostly non-coding RNA (ncRNA).

To test which RNAP transcribes *Ube3a-ATS*, primary neuronal cultures derived from neonatal wild-type (WT) mice were treated with a low concentration of α-amanitin (5 μg/ml), an RNAPII-specific inhibitor, for 48 h. Samples with and without drug treatment were collected and compared by quantitative PCR (q-PCR) (Fig. 1A). The 18S ribosomal RNA was used as the internal control. The level of *26S* rRNA, which is transcribed by RNAPI, was not affected by the drug treatment. Transcription of *5S* rRNA and *U6* snRNA, two known RNAPIII transcripts, appeared to be increased several fold after treatment which may reflect a true relative change or an artifact due to normalization. *Actb* and *Ube3a* are protein-coding genes known to be transcribed by RNAPII. As expected, their transcription was sensitive to α-amanitin treatment, and expression was decreased by 50–70%. The two antisense RNAs, *Ube3a-ATS* and *Airn*, were also down-regulated significantly by α-amanitin treatment, indicating that they are transcribed by RNAPII. Three sets of primers targeting various regions of *Ube3a-ATS* were used to measure its expression (Supplementary Material, Fig. S1). All primer sets give similar results.

RNAPII transcripts are generally poly-adenylated with the exception of those from histone genes. To test if *Ube3a-ATS* is poly-adenylated, mRNA purified by oligo(dT) beads was compared with total RNA (Fig. 1B). As measured by q-PCR, protein-coding genes (*Gapdh, Ube3a* and *Actb*) had poly-adenylation rates varying from 20 to 70% (normalized to *Pgk1*, which was set as 100%), whereas only trace amount of rRNA and snoRNA (0.1% of *18S* and 0.4% of *MBII-52*) can be detected in the polyA+ sample. Poly-adenylation status along the hypothetical long transcript *LNCAT* was also examined. Surprisingly, although *Snrpn* transcripts including both major and upstream exons had a poly-adenylation rate of 46–57%, only 2–6% of the downstream transcripts (*Ipw* and *Ube3a-ATS*) were shown to be poly-adenylated, implying that different portions of the transcript are processed differently and separately. Therefore, the majority of *Ube3a-ATS* transcripts were not poly-adenylated. Similarly, another imprinted antisense RNA *Airn* also showed a poly-adenylation rate of only 3.9% in our analysis.

Typical protein-coding transcripts are transported into the cytoplasm to be translated. To examine the subcellular localization of *Ube3a-ATS*, nuclear and cytoplasmic RNA was extracted from primary neuronal cultures, and the ratio of the two was measured by q-PCR (Fig. 1C). Transcripts for protein-coding genes, like *Ube3a* and *Actb*, both had cytoplasmic-to-nuclear (c/n) ratios closer to or higher than 1 (*Pgk1* was set to have the ratio of 1, *Ube3a* had a ratio of 0.61 and *Actb* had a ratio of 1.62). In contrast, nuclear-retained RNAs, like the *45S* precursor rRNAs and imprinted ncRNA *Airn*, showed c/n ratios much smaller than 1 (0.01 for *45S* and 0.04 for *Airn*). Similar to these two transcripts, *Ube3a-ATS* had a c/n ratio of 0.01–0.03, suggesting that it was localized in the nucleus.

Finally, we measured the half-life of *Ube3a-ATS* by treating primary neuronal cultures with the RNAP inhibitor actinomycin D (ActD, 10 μg/ml) and quantifying the remaining amount of the transcripts over a 48-h period (Fig. 1D). The transcripts of *c-Myc* were extremely unstable and were completely degraded within 4 h (dashed-dotted line in Fig. 1D, estimated half-life <2 h). *Ube3a-ATS* was more stable with an estimated half-life of ~4 h (solid lines). However, this was much shorter than other protein-coding transcripts tested (dashed lines, *Ube3a* ~48 h and *Actb* ~24 h). It was even shorter than the other imprinted antisense RNA *Airn* (half-life ~12 h).

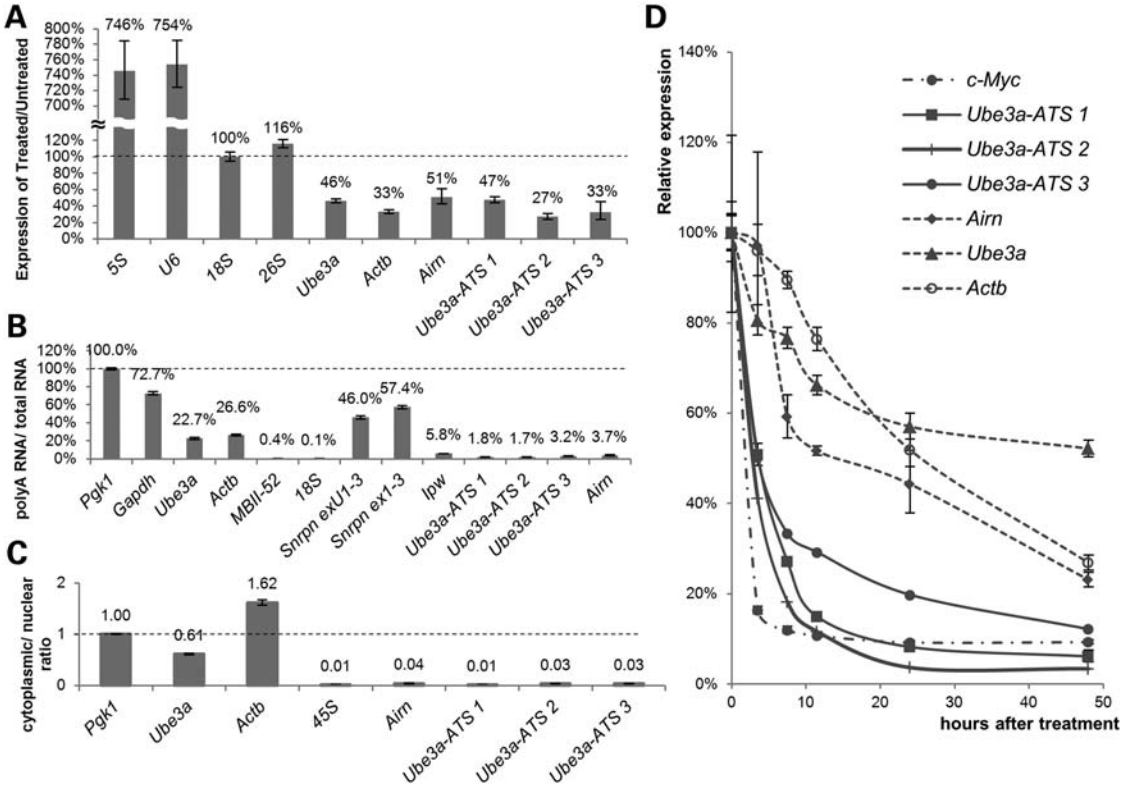

Figure 1. *Ube3a-ATS* is an atypical RNAPII transcript. (**A**) To test if *Ube3a-ATS* was transcribed by RNAPII, primary neuronal cultures were treated with RNAPII inhibitor α-amanitin (5 μg/ml) for 48 h. Expression levels were measured by q-PCR and normalized to *18S* rRNA. (**B**) To test if *Ube3a-ATS* was poly-adenylated, mRNA purified with oligo(dT) beads was compared with total RNA by q-PCR. *Pgk1* was used as the reference control and its poly-adenylation rate was set as 100%. Protein-coding genes, such as *Gapdh* and *Actb*, served as positive controls for poly-adenylated genes, and ncRNAs, such as snoRNA *MBII-52* and rRNA *18S*, were negative controls for non-poly-adenylated genes. (**C**) To test the subcellular localization of *Ube3a-ATS*, total RNAs were extracted from nuclear and cytoplasmic fractions of primary neuronal cultures, and the ratio of c/n was measured by q-PCR. *Pgk1* was used as the reference control and its c/n ratio was set as one. Protein-coding transcripts such as *Ube3a* and *Actb* and nuclear-retained RNAs like *45S* rRNA and *Airn* were included as controls. (**D**) To measure the half-life of *Ube3a-ATS*, primary neuronal cultures were treated with 10 μg/ml of ActD and harvested at various time points. RNA was extracted and analyzed by q-PCR. All transcripts were normalized to *18S* rRNA. Transcripts are indicated as follows: dashed-dotted line for *c-Myc*, dashed lines for *Ube3a*, *Actb* and *Airn*, solid lines for *Ube3a-ATS.* All the experiments were repeated at least two times with a representative result showing here. Error bars represent the standard error of means of three technical replicates.

In summary, *Ube3a-ATS* was an atypical RNAPII transcript. It was transcribed by RNAPII, localized in the nucleus and was not poly-adenylated. It was relatively unstable with a half-life shorter than most RNAPII transcripts tested. All of these features differ from typical RNAPII transcripts, but are similar to *Airn* and *Kcnq1ot1*, the other two imprinted antisense RNAs (21,22), implying a possible convergent function and mechanism in the imprinting process.

Paternal *Ube3a* is activated by *Ube3a-ATS* promoter deletion

It was reported previously that the paternal deletion of a 35-kb region of the *Snrpn* promoter, exon1–6, and its 5′ upstream region leads to *Ube3a-ATS* suppression, coupled with paternal *Ube3a* activation (27). However, since the *Snrpn* promoter is located within the PWS-IC, it is difficult to separate the two functional domains for imprinting control versus promoter activity. In the 35-kb deletion mice, it cannot be distinguished if the activation of paternal *Ube3a* was caused by the depletion of the *Ube3a-ATS* transcript or the deletion of *cis*-regulatory elements such as the PWS-IC.

Two mouse models carrying different sizes of deletions over the *Snrpn* major promoter were generated previously (31). The smaller deletion ($del^{0.9}$) is 912-bp long and removes *Snrpn* exon1 and a small portion of the DMR1 (Fig. 2A). Mice with this deletion inherited paternally were reported to have normal DNA methylation patterns for *Snrpn* by methylation-sensitive enzyme digestion. Decreased expression of *Snrpn* and an overall normal phenotype were also reported in this mutant (31). In contrast, the larger deletion ($del^{4.8}$) covers 4.8 kb including most of DMR1. Paternal inheritance of this 4.8-kb deletion leads to abnormal DNA methylation of *Ndn* and perinatal lethality and growth retardation similar to other PWS mouse models (31). Given these results, we hypothesized that $del^{0.9}$ on the paternal chromosome only affects the activity of *Snrpn* promoter, but not PWS-IC, making it an ideal model to study the role of *Ube3a-ATS*.

To test this, the DNA methylation of *Snrpn* intron1 (immediate downstream of the deletion region, Supplementary Material, Fig. S2) was measured by bisulfite sequencing of cortical DNAs extracted from the cerebral cortex of WT and $del^{+/0.9}$ mice. These mice are the F1 generation of $del^{+/0.9}$

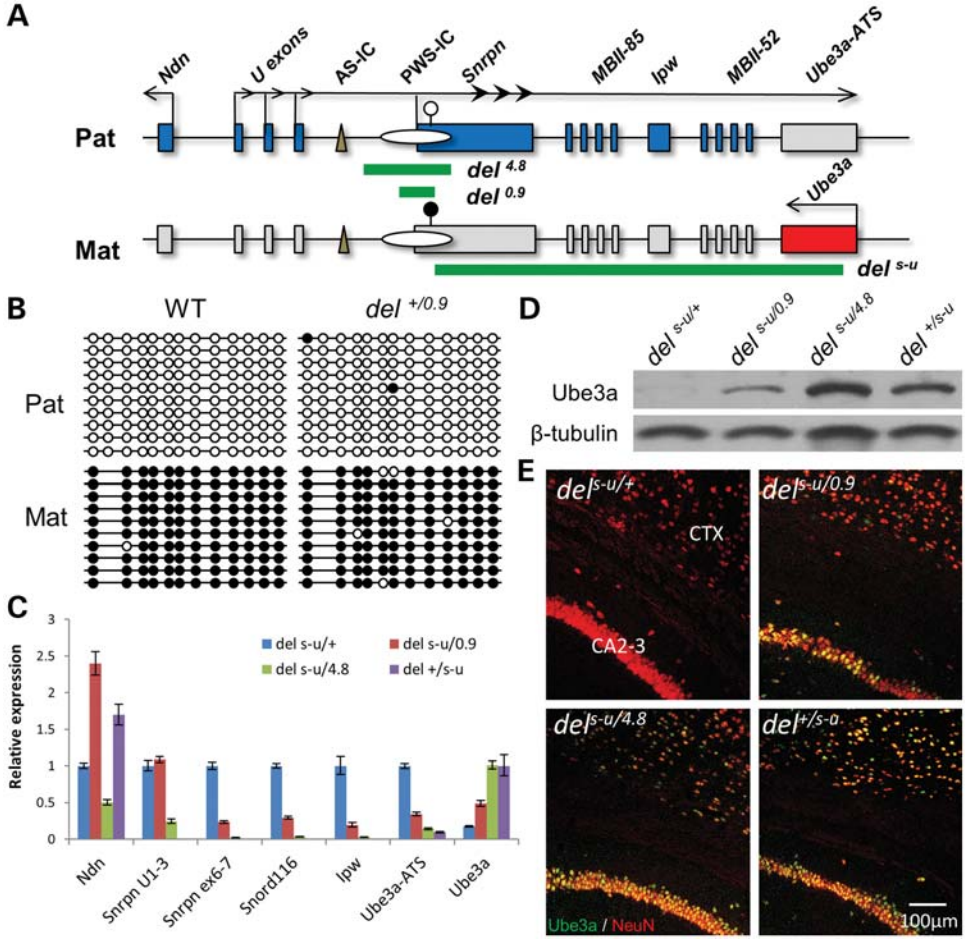

Figure 2. Both 0.9- and 4.8-kb deletions at the *Snrpn* promoter activate the paternal expression of *Ube3a*. (**A**) The PWS/AS imprinted region is shown with paternally expressed genes highlighted in blue, maternally expressed genes in red and silenced genes in gray (not drawn to scale). *Ube3a-ATS* is proposed to be processed from the same precursor encoding *Snrpn*, which has multiple upstream promoters. The major promoter is located within PWS-IC. Regions deleted in each mutant allele are shown by the green bars: $del^{4.8}$ covers most of the PWS-IC; $del^{0.9}$ covers the *Snrpn* major promoter and a small part of PWS-IC; del^{s-u} is a deletion from *Snrpn* to *Ube3a*. The open circle represents unmethylated status and the closed circle represents methylated status. Pat, paternal; Mat, maternal. (**B**) Bisulfite sequencing of *Snrpn* intron1 downstream of the 0.9-kb deletion region was performed with DNA extracted from the cerebral cortex of WT and $del^{+/0.9}$ mice at P14. Mice analyzed were the F1 generation of a cross between male C57BL/6J $del^{+/0.9}$ mice and female CAST.chr7 WT mice. Clones representing the maternal allele were distinguished by the conversion of a CpG dinucleotide (CG > AA). A total of 13 CpG dinucleotides were analyzed with open circles for unmethylated CpG and closed circle for methylated CpG. Ten random clones from each allele were shown with each line representing sequences from one clone. (**C**) The expression pattern of selected genes located in the PWS/AS region were compared in newborn mouse brains of $del^{s-u/+}$, $del^{s-u/0.9}$, $del^{s-u/4.8}$ and $del^{+/s-u}$ mutants by q-PCR. All transcripts were normalized to the internal control of *Pgk1*. For better illustration, $del^{+/s-u}$ was used as the reference when the *Ube3a* level was plotted, and $del^{s-u/+}$ was the reference when plotting the rest of the genes. Three biological replicates were performed with one representative result shown here. Error bars represent the standard error of means from three technical repeats. (**D**) Western blot was performed with proteins extracted from newborn mouse brains of $del^{s-u/+}$, $del^{s-u/0.9}$, $del^{s-u/4.8}$ and $del^{+/s-u}$ mutants. β-Tubulin was used as the loading control. (**E**) Brain sections from 1-month-old mice were immunostained with anti-Ube3a (green) and anti-NeuN (red). Expression of paternal Ube3a was detected in cortical and hippocampal neurons in the $del^{s-u/0.9}$ and $del^{s-u/4.8}$ mutants. Ctx, cerebral cortex; WT, wild-type.

C57BL/6J male mice and CAST.chr7 female mice, which is a strain congenic for *M. musculus castaneus* chromosome 7 on a C57BL/6J background (32). Polymorphisms between the two strains were used to distinguish the parental alleles during sequencing analysis. As expected, the paternal allele of *Snrpn* in the $del^{+/0.9}$ mice remains fully unmethylated, as in the WT mice (Fig. 2B).

As another read-out of the activity of the IC, the expression of those transcripts regulated by the PWS-IC was then studied. To eliminate any interference from the maternal chromosome, male mice of $del^{0.9/0.9}$ or $del^{4.8/4.8}$ were crossed with female mice carrying a large genomic deletion from *Snrpn* to *Ube3a* (del^{s-u}) (33) to generate $del^{s-u/0.9}$ or $del^{s-u/4.8}$ mice. As expected, $del^{s-u/4.8}$ mice showed reduced expression of all the transcripts tested, including *Ndn* and all genes processed from *LNCAT*, compared with $del^{s-u/+}$ (Fig. 2C) confirming the previous conclusion that $del^{4.8}$ mutation impairs PWS-IC function (31). However, in $del^{s-u/0.9}$ mice, only genes that are directly transcribed from the major promoter (*Snrpn* ex6-7, *Ipw* and *Ube3a-ATS*) were significantly down-regulated. Upstream transcripts, including *Ndn* and *Snrpn* exU1-3, did not decrease (Fig. 2C), suggesting that the 0.9-kb deletion affected only the *Snrpn* major promoter, but not the PWS-IC. DNA methylation and gene expression data

combined confirm the previous conclusion that the 0.9-kb deletion over the *Snrpn* promoter does not abolish PWS-IC activity, while the 4.8-kb deletion does.

It has been suggested previously that the expression of *Ube3a-ATS* initiates from the *Snrpn* upstream promoters (25). However, we found that *Ube3a-ATS* expression was decreased by 50% in the $del^{s\text{-}u/0.9}$ mutant (Fig. 2C), implying that about half of *Ube3a-ATS* was transcribed from the *Snrpn* major promoter. Interestingly in this mutant, the expression level of paternal *Ube3a* was found to be up-regulated to about half of the maternal level, as revealed by q-PCR and western blot (Fig. 2C and D). Immunostaining against Ube3a in brain sections further confirmed the expression of paternal Ube3a in all brain regions, with the highest level in neurons of neocortex, hippocampus and Purkinje cells of cerebellum, similar to that of maternally expressed Ube3a (Fig. 2E and Supplementary Material, Fig. S3). The switch-on of paternal Ube3a by the deletion of the *Snrpn/Ube3a-ATS* promoter ($del^{0.9}$) strongly supports a direct role of *Ube3a-ATS* in mediating *Ube3a* imprinting, although the possibility cannot be ruled out that the 912-bp deleted region may contain other *cis*-regulatory elements. It was also noted that the activation of paternal *Ube3a* was incomplete in $del^{s\text{-}u/0.9}$ compared with $del^{s\text{-}u/4.8}$ mutants (Figs. 2C and 2D). This may due to remaining expression of *Ube3a-ATS* transcribed from the *Snrpn* upstream promoters in the $del^{s\text{-}u/0.9}$ mutants. In contrast, *Ube3a-ATS* expression is completely abolished in the $del^{s\text{-}u/4.8}$ mutants since *Snrpn* upstream promoters were inactivated by the imprinting defect. Consequently, paternal *Ube3a* was activated completely.

In summary, we demonstrated that (i) the 0.9-kb deletion affected only the promoter activity of *Snrpn*, but not PWS-IC; (ii) at least 50% of *Ube3a-ATS* was transcribed from the *Snrpn* major promoter; (iii) a decreased level of *Ube3a-ATS*, resulting from its promoter deletion, was sufficient to unsilence paternal *Ube3a*.

Early termination of *Ube3a-ATS* activates paternal *Ube3a* in cultured differentiated neurons

Activation of paternal *Ube3a* in the mouse model of $del^{s\text{-}u/0.9}$ strongly supports the role of *Ube3a-ATS* in silencing *Ube3a in cis*. However, in this mutant, a small portion of PWS-IC was deleted, and many transcripts processed from *LNCAT* in addition to *Ube3a-ATS* were also down-regulated. Whether the reduction in *Ube3a-ATS* transcription alone is sufficient to activate paternal *Ube3a* remains unknown. This is important for understanding the imprinting mechanism of *Ube3a* as well as for designing therapeutic strategies for Angelman syndrome.

To address this question, a transcriptional termination cassette consisting of a splicing acceptor, a triple polyA signal derived from SV40, and a phosphoglycerate kinase (PGK)-neomycin selection marker was inserted 11.9 kb downstream of *Ube3a* via genetic recombineering (Fig. 3B, Supplementary Material, Fig. S4A). To avoid transcription initiation of *Ube3a-ATS* by the PGK promoter, the PGK-neo gene was oriented in the antisense direction of *Ube3a-ATS*. In order to identify the parental alleles, $Ube3a^{+/YFP}$ male mice with a yellow fluorescence protein (YFP) tag in the 3′UTR of *Ube3a* (12) were crossed with WT female mice to generate $Ube3a^{+/YFP}$ ES cells (Fig. 3A). These cells were later used for electroporation and homologous recombination. An $Ube3a^{YFP/+}$ clone was also established from the reciprocal cross as a positive control. After screening by Southern blot, three clones were identified with the insertion of the stop cassette on the paternal chromosome (i.e. *in cis* of the *YFP* allele, annotated as $Ube3a^{+/YFP;stop}$), and one clone was identified with the insertion on the maternal chromosome (i.e. *in trans* of the *YFP* allele, annotated as $Ube3a^{stop/YFP}$) (Supplementary Material, Fig. S4B and C).

Since *Ube3a* imprinting status is only established in neurons, ES cell clones of $Ube3a^{YFP/+}$, $Ube3a^{+/YFP}$, $Ube3a^{stop/YFP}$ and $Ube3a^{+/YFP;stop}$ were differentiated into neurons in culture (Fig. 3A) using a protocol modified from Bibel *et al.* (34). The success of neuronal differentiation was confirmed by the morphology of the cells and up-regulation and positive staining of the neuronal marker Map2 (Fig. 3D and Supplementary Material, Fig. S5). Expression of *Ube3a-YFP* sense and antisense was then measured in those differentiated cells by q-PCR (primer design was as shown in Supplementary Material, Fig. S6). As expected, the insertion of the stop cassette on the paternal chromosome decreased the expression of $Ube3a\text{-}ATS^{YFP}$ ($P = 0.001$), while insertion on the maternal chromosome did not (Fig. 3C). The paternal expression of $Ube3a^{YFP}$, on the other hand, was found to be activated in $Ube3a^{+/YFP;stop}$ neurons ($P = 0.001$), but not in $Ube3a^{stop/YFP}$ neurons. The expression level of activated paternal $Ube3a^{YFP}$ was comparable with the maternally expressed $Ube3a^{YFP}$ in $Ube3a^{YFP/+}$ neurons, indicating a complete unsilencing effect. Immunostaining with anti-YFP further confirms the activation of paternal $Ube3a^{YFP}$ in $Ube3a^{+/YFP;stop}$ neurons ($P < 0.001$, Fig. 3D and E). Therefore, the depletion of *Ube3a-ATS* by early termination of its expression is sufficient to activate paternal *Ube3a*.

Detection of *Ube3a-ATS* by strand-specific microarray

To further characterize *Ube3a-ATS*, a strand-specific microarray was designed for the mouse *Snrpn-Ube3a* region, with probes targeting both plus and minus strands. In mice, *Ube3a* is annotated on the plus strand, which is defined to have small genomic coordinate at 5′-end and large coordinate at 3′-end. *Snrpn*, snoRNAs *MBII-52/85* and *Ube3a-ATS* are annotated on the minus strand. The array successfully detected exons of *Ube3a* and *Snrpn* (Fig. 4A, left panel and Supplementary Material, Fig. S7). The validity of this analysis was further demonstrated by decreased *Ube3a* exonic detection in the AS mouse model ($del^{s\text{-}u/+}$) (over the genomic deletion region shown by the green bar in Fig. 4A) and by the absence of *Snrpn* in the PWS mouse model ($del^{+/s\text{-}u}$) (Supplementary Material, Fig. S7). The low but detectable expression level of *Ube3a* in the AS mouse model is consistent with the previous observation that it is biallelically expressed at a low level in some of the glial cells (11,12). On the minus strand of the *Ube3a* locus, an antisense transcript was detected spanning the entire region (Fig. 4A, right panel). This corresponded to *Ube3a-ATS*. It was detected in both the WT and AS mice, but was completely absent in the PWS mouse. This is in accordance with previous conclusion that *Ube3a-ATS* is completely silenced in the brain and expressed only from the paternal chromosome.

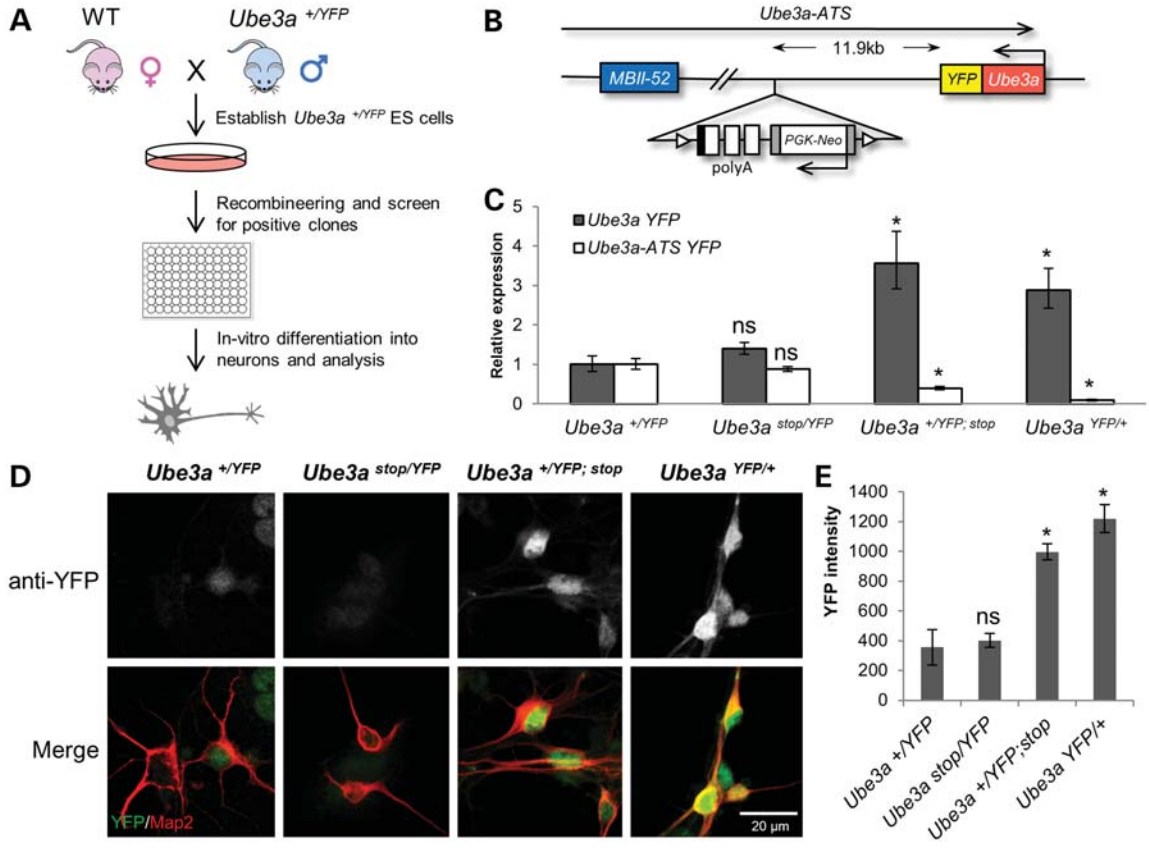

Figure 3. Early termination of *Ube3a-ATS* activates paternal *Ube3a* in cultured differentiated neurons. (**A**) Male $Ube3a^{+/YFP}$ mice were crossed with female WT mice to generate primary ES cells of $Ube3a^{+/YFP}$. The ES cells were then electroporated with a targeting vector, selected with neomycin and screened for positive clones by Southern blot. Clones with *stop* allele inserted in *cis* or in *trans* of the $Ube3a^{YFP}$ allele were also identified by Southern blot. The *cis* and *trans* clones ($Ube3a^{+/YFP;stop}$ and $Ube3a^{YFP/stop}$), together with control clones (negative control of $Ube3a^{+/YFP}$ and positive control of $Ube3a^{YFP/+}$), were differentiated into neuronal linage and harvested for RNA and protein analysis. (**B**) The transcription termination cassette was engineered into the genome 11.9-kb downstream of *Ube3a.* The cassette consists of a pair of loxP sites (triangles), a splicing donor (black box), a triple polyA signal derived from SV40 (white boxes) and FRT-flanked PGK-neomycin (white box flanked with gray boxes). (**C**) Using q-PCR, the levels of $Ube3a^{YFP}$ and $Ube3a\text{-}ATS^{YFP}$ were determined in differentiated neuronal cells of $Ube3a^{YFP/+}$, $Ube3a^{+/YFP}$, $Ube3a^{stop/YFP}$ and $Ube3a^{+/YFP;stop}$ genotypes. Both transcripts were normalized to the internal control of *Pgk1.* (**D**) Differentiated neuronal cells were immunostained with anti-YFP and neuronal marker anti-Map2. The top panels show anti-YFP signal only and the bottom panels are merge of anti-YFP (green) and anti-Map2 (red). (**E**) YFP intensity was quantified in Map2 positive cells of four different clones by ImageJ. Error bars represent the standard error of means. Statistical analysis was performed with Student's *t*-test comparing the sample with the control of $Ube3a^{+/YFP}$. ns, not significant; $^{*}P < 0.01$.

Samples from $del^{s\text{-}u/0.9}$ and $del^{s\text{-}u/4.8}$ mutant mice were also analyzed by the microarray (Fig. 4A). Consistent with q-PCR results, the expression of *Ube3a-ATS* was decreased ~50% in the $del^{s\text{-}u/0.9}$ mutant and was barely detectable in the $del^{s\text{-}u/4.8}$ mutant (Fig. 4A). Correspondingly, the expression of paternal *Ube3a* was activated in a 'dosage-dependent' manner.

To further define whether *Ube3a-ATS* is poly-adenylated or not, cDNAs generated from polyA+ RNA from WT mice was hybridized to the same microarray (Fig. 4A, lowest panels). After being normalized to the control genes (average intensity of *Pgk1*, *Gapdh*, *Tfrc* and *Actb*), exons of both *Ube3a* and *Snrpn* were detected, and the relative signal intensity was comparable with that using total RNA as the input (Fig. 4A and Supplementary Material, Fig. S7). However, only a weak signal of *Ube3a-ATS* was detected, suggesting that *Ube3a-ATS* is mostly not poly-adenylated.

Considering that paternal $del^{0.9}$ or $del^{4.8}$ mutation eliminates part or all of *Ube3a-ATS* expression, we argue that the difference between $del^{s\text{-}u/+}$ and $del^{s\text{-}u/0.9}$ or $del^{s\text{-}u/4.8}$ should represent a more accurate measure of *Ube3a-ATS*, as this removes most of the background noise due to bad probes. Therefore, the signal intensity of sample $del^{s\text{-}u/0.9}$ or $del^{s\text{-}u/4.8}$ was subtracted from that of sample $del^{s\text{-}u/+}$ (Fig. 4B). One observation based on the subtraction analysis is the lack of the exon–intron structure of *Ube3a-ATS*. This indicates that *Ube3a-ATS* was either not spliced or spliced in a heterogeneous manner, which cannot be distinguished here. Previous northern blot of *Ube3a-ATS* revealed a pattern of smearing rather than single or multiple bands (30). Exons and splice junctions of *Ube3a-ATS* have been identified before by RT–PCR (25), suggesting that at least a portion of the antisense RNA is spliced.

The transcription of *Ube3a-ATS* was shown to be active across the entire gene locus of *Ube3a* (Fig. 4B). This is consistent with previous identification of human expressed sequence tags mapping to intron 1, intron 7 and the 3′-region

of *UBE3A* in the antisense orientation (24). The termination site of *Ube3a-ATS* is likely to be located ~40 kb beyond the *Ube3a* transcription start site (TSS) as revealed by the microarray, suggesting the active transcription of *Ube3a-ATS* at the *Ube3a* promoter. Analysis with q-PCR confirmed the high expression of *Ube3a-ATS* at the 500-bp upstream of the *Ube3a* TSS (Supplementary Material, Fig. S8). The expression level dropped dramatically at loci located 2 kb upstream and beyond. However, the difference between WT and the $del^{+/0.9}$ mutant remained significant for all the regions tested, indicating that there was still residual expression of *Ube3a-ATS* beyond the 2-kb upstream of the *Ube3a* TSS. Consistent with our finding, Numata *et al.* (35) also found that mouse *Ube3a-ATS* extends beyond the *Ube3a* TSS as revealed by their highly parallel single-nucleotide polymorphism (SNP) genotyping.

DISCUSSION

ncRNA *Ube3a-ATS* mediates imprinting of *Ube3a*

A possible role of *Ube3a-ATS* in silencing paternal *Ube3a* has been proposed in the past. In many observations, the expression of *Ube3a* and *Ube3a-ATS* is negatively correlated (11,27,28). However, a causal relationship between the two has not been established. In this research, we reported a new mouse model and cell culture model which are powerful tools in studying the role of *Ube3a-ATS* in *Ube3a* imprinting.

In mice with the 0.9-kb genomic deletion inherited paternally, *Ube3a-ATS* expression was decreased as a result of the *Snrpn/Ube3a-ATS* promoter deletion. Consistent with the hypothesis that *Ube3a-ATS* silences *Ube3a in cis*, paternal *Ube3a* was found to be activated partially in the mutant mice. A previous mouse model with a 35-kb deletion over *Snrpn* exon1–6 and its 5′ upstream region was reported to have activated paternal *Ube3a* and repressed *Ube3a-ATS*. However, it was inconclusive whether unsilencing of paternal *Ube3a* was caused directly by the loss of *Ube3a-ATS* or indirectly through the deletion of PWS-IC. Our 0.9-kb deletion only disrupted the activity of the *Snrpn* promoter without significant effects on the PWS-IC, as indicated by the normal DNA methylation pattern of *Snrpn* (Fig. 2B) and the unaffected expression of *Ndn* and *Snrpn* upstream exons (Fig. 2C). This, for the first time, demonstrated that a reduction in *Ube3a-ATS* expression, with no disruption of PWS-IC, can lead to the biallelic expression of *Ube3a*.

The cell culture model of $Ube3a^{+/YPF;stop}$ carries a transcriptional termination signal inserted downstream of *Ube3a* on the paternal chromosome. It gives a cleaner genetic background as it does not remove any genetic material and changes the expression of only *Ube3a-ATS* but not *Snrpn* and the snoRNAs. The activation of paternal $Ube3a^{YFP}$ in this model definitively demonstrated that the elimination of *Ube3a-ATS* by genetic manipulation is sufficient to unsilence paternal *Ube3a*. This evidence not only reenforces the critical role of *Ube3a-ATS* in *Ube3a* imprinting, but also provides a proof-of-principle for future therapeutic approaches to Angelman syndrome.

One of the important questions remaining to be addressed is whether the *cis* silencing of *Ube3a* by *Ube3a-ATS* is caused by the presence of the antisense RNA itself or by the action of transcription through the locus. This question is hard to resolve because it is difficult to separate the action of transcription from the product of transcription. In one study on another imprinted antisense RNA *Kcnq1ot1*, a 3′-UTR element of a quickly degraded mRNA *c-fos* was cloned downstream of the *Kcnq1ot1* promoter. With this strategy using episomal expression, the RNA amount of *Kcnq1ot1* was reduced due to more rapid turnover time while transcription was unaffected (22). Complete loss of silencing of the non-overlapping hygromycin gene was observed in the fosUTR+ construct, but not in the fosUTR− control, indicating that the RNA *per se*, rather than its act of transcription, is crucial for its bidirectional silencing. Another complex study on X-inactivation with the expression of the truncated endogenous *Tsix* and exogenous *Tsix* cDNA led to the opposite conclusion, suggesting that transcription of *Tsix* across the *Xist* locus is necessary to block *Xist* up-regulation (36). Similar attempts to distinguish the presence of antisense RNA versus the act of transcription may be useful in studying *Ube3a-ATS*, although its large size may make such studies more difficult.

Angelman syndrome patients can be subdivided into five types based on their molecular mechanisms: maternal interstitial deletion of 15q11-q13 (60–75%), paternal uniparental disomy (2–5%), imprinting defects with or without microdeletions over IC (2–5%), mutation in *UBE3A* gene (10–20%) and unknown mechanism, which may include some cases of the abnormal expression of *UBE3A* and some misdiagnoses where *UBE3A* is not involved in the pathogenesis (3,6,7,13,37). Based on our findings in mice that *Ube3a-ATS* mediates the silencing of paternal *Ube3a*, we raise the possibility that part of patients with unknown mechanism may have the biallelic expression of *UBE3A-ATS* in the brain, and subsequently, the loss of maternal *UBE3A* expression. Possible mechanisms may include ectopic promoter insertion at the locus of *UBE3A-ATS* or translocation between *UBE3A* and another transcriptional active locus.

Ube3a-ATS is a large ncRNA similar to *Airn* and *Kcnq1ot1*

As a large ncRNA, *Ube3a-ATS* is very poorly characterized. To facilitate future studies on its function and potential development as the therapeutic target, we investigated some of its basic features. By comparing with the other two imprinted antisense RNAs, *Airn* and *Kcnq1ot1*, we found that all three are very similar to each other (Table 1). They are all transcribed by RNAPII, but do not have coding sequence. All three RNAs are mainly localized in the nucleus, consistent with their role in down-regulating gene expression of the sense transcript. *Ube3a-ATS* has been reported before to be localized primarily in cytoplasm by *in situ* hybridization in mouse brain sections (26). The discrepancy might arise from different methods used. It was reported before that both *Airn* and *Kcnq1ot1* are poly-adenylated. However, this conclusion was drawn based on data obtained from rapid amplification of cDNA 3′ ends using oligo(dT) primers (22,38). We measured poly-adenylation by comparing purified polyA+ RNA with total RNA and found that only 4.0 and 1.8% of *Airn* and *Ube3a-ATS*, respectively, were poly-adenylated. These

Table 1. Comparison among three large ncRNAs involved in imprinting

	Ube3a-ATS	*Airn*	*Kcnq1ot1*
RNAP	RNAPII (Fig. 1A)	RNAPII (21)	RNAPII (22)
Size	>1000 kb (genomic) (25)	108 kb (21,38)	80–120 kb (22,48)
Splicing	No exon–intron structure as shown by the microarray (Fig. 4B). Exon–exon junction was identified before (25)	Mostly unspliced; spliced isoforms were identified. The abundance of steady-state spliced relative to unspliced was 23–44% (21)	No evidence of splicing (21,22)
Poly-adenylation	Low percentage of poly-adenylation (Fig. 1B)	Yes (21), but we found low poly-adenylation rate in mouse brain (Fig. 1B)	A polyA site was identified the 121-kb downstream of TSS (48)
Subcellular localization	Nucleus (Fig. 1C)	Unspliced form is localized in nucleus (21)	Nucleus (48)
Stability (half-life)	~4 h (Fig. 1D)	1.6 h (38)	3.4 h (48); 4.73 h (22)
Function	Truncation of Ube3a-ATS leads to the activation of Ube3a (Fig. 3)	Truncation of Airn leads to activation of Igf2r, Slc22a2 and Slc22a3 (19)	Truncation of Kcnq1ot1 leads to the activation of all seven genes tested in the imprinting cluster (20)

rates are much lower than typical protein-coding genes, but slightly higher than other ncRNAs like rRNAs or snoRNAs. The low poly-adenylation rates of *Ube3a-ATS* and *Airn* may also account for their low stability, as indicated by the short half-life. The half-life we measured for *Airn* is longer than that previously reported (21). This may due to different metabolic rates between the brain and the mouse embryonic fibroblasts in the previous study. *Kcnq1ot1*, although not measured in our study, was also reported to have a short half-life ~4 h (22).

Recently, *cis*-acting long ncRNAs have emerged as a new class of ncRNAs distinctive from well-known *trans*-acting small ncRNAs (39). Interestingly, many imprinted gene clusters contain such long ncRNAs with their transcription initiated from the IC. Among them, *Airn* and *Kcnq1ot1* are the two that have been studied most extensively. The mechanism whereby these RNAs silence the corresponding *cis* transcripts remains unclear. Proposed models include transcriptional interference between the two overlapping transcripts especially at promoters, RNA interference caused by bidirectional transcription and chromatin modification by antisense RNA in a chromatin coating manner similar to *Xist* (16,17). *Ube3a-ATS* shows high similarity with *Airn* and *Kcnq1ot1*. Similar mechanism might be involved in *Ube3a-ATS* mediated gene silencing, although further investigations are needed.

Transcription initiation, termination and splicing of *Ube3a-ATS*

Ube3a-ATS is hypothesized to be part of the large transcript *LNCAT*. Previous studies on its expression patterns in mice have suggested that the antisense transcript is more likely to be regulated by *Snrpn* upstream exons, rather than exon1 (25). However, we found that in $del^{s\text{-}u/0.9}$ mice with paternal *Snrpn* exon1 deleted, the *Ube3a-ATS* level was decreased by 50% with no reduction in *Snrpn* U exons (Fig. 2C), suggesting that at least half of *Ube3a-ATS* transcripts were contributed by the *Snrpn* major promoter. The remaining amount of the transcripts may be transcribed from the U exons, as *Ube3a-ATS* expression was completely abolished in $del^{s\text{-}u/4.8}$ mice. The conclusion that part of *Ube3a-ATS* transcribes from the *Snrpn* major promoter is not contradictory to the fact that *Ube3a-ATS* is neuronal-specific while *Snrpn* is ubiquitously expressed. It is possible that in non-neuronal cells *Snrpn* is mainly transcribed from the major promoter and encodes only *Snrpn*, while in neurons all the *Snrpn* promoters, including both the major promoter and the upstream promoters, are active and give rise to the longer transcript, *LNCAT* (*Snrpn*, snoRNAs, *Ipw* and *Ube3a-ATS*). The transition between the two states might be controlled by some neuronal-specific regulatory elements.

The precise termination site of *Ube3a-ATS* has not been investigated before. Our strand-specific microarray provides some information on this question. *Ube3a-ATS* was detected over the entire gene body of *Ube3a*. The signal intensity decreased gradually when it reaches the 5′-portion of the sense *Ube3a* locus but was not completely down to the background level until ~40 kb upstream of the *Ube3a* TSS (Fig. 4B). Therefore, at least some of *Ube3a-ATS* transcripts overlap the promoter region of *Ube3a*. Overlapping between antisense RNA and the TSS of the sense gene may create a conflict for the moving RNAPs in both directions and therefore is viewed as a prerequisite for the transcriptional interference mechanism. The fact that *Ube3a-ATS* transcribed through the *Ube3a* promoter region fits into this model. The data also suggest that instead of one single termination site, there might be multiple termination sites of *Ube3a-ATS* spanning up to 40 kb beyond the *Ube3a* promoter. The adjacent gene *ATP10A/Atp10a* was initially reported to be imprinted in human (40,41), but recent data from mice suggested that it is biallellically expressed in most brain regions (42,43). The fact that *Ube3a-ATS* terminated shortly beyond the *Ube3a* and did not extend into *Atp10a* implies a functional role of *Ube3a-ATS* in *Ube3a* imprinting and that the process is tightly regulated.

Splicing of *Ube3a-ATS* was not specifically studied in this research. Our strand-specific microarray shows no clear exon–intron boundary for the antisense RNA. Exon–exon boundaries have been reported before by RT–PCR (25), and we were able to confirm the reported junction (data not shown). However, the relative ratio of the specific spliced isoform versus unspliced isoform was found to be low. Therefore, in our studying, the quantification of *Ube3a-ATS* was all carried out with primers amplifying unspliced isoform. It remains possible that some features of the spliced *Ube3a-ATS* isoform may be different from the unspliced form that we studied here.

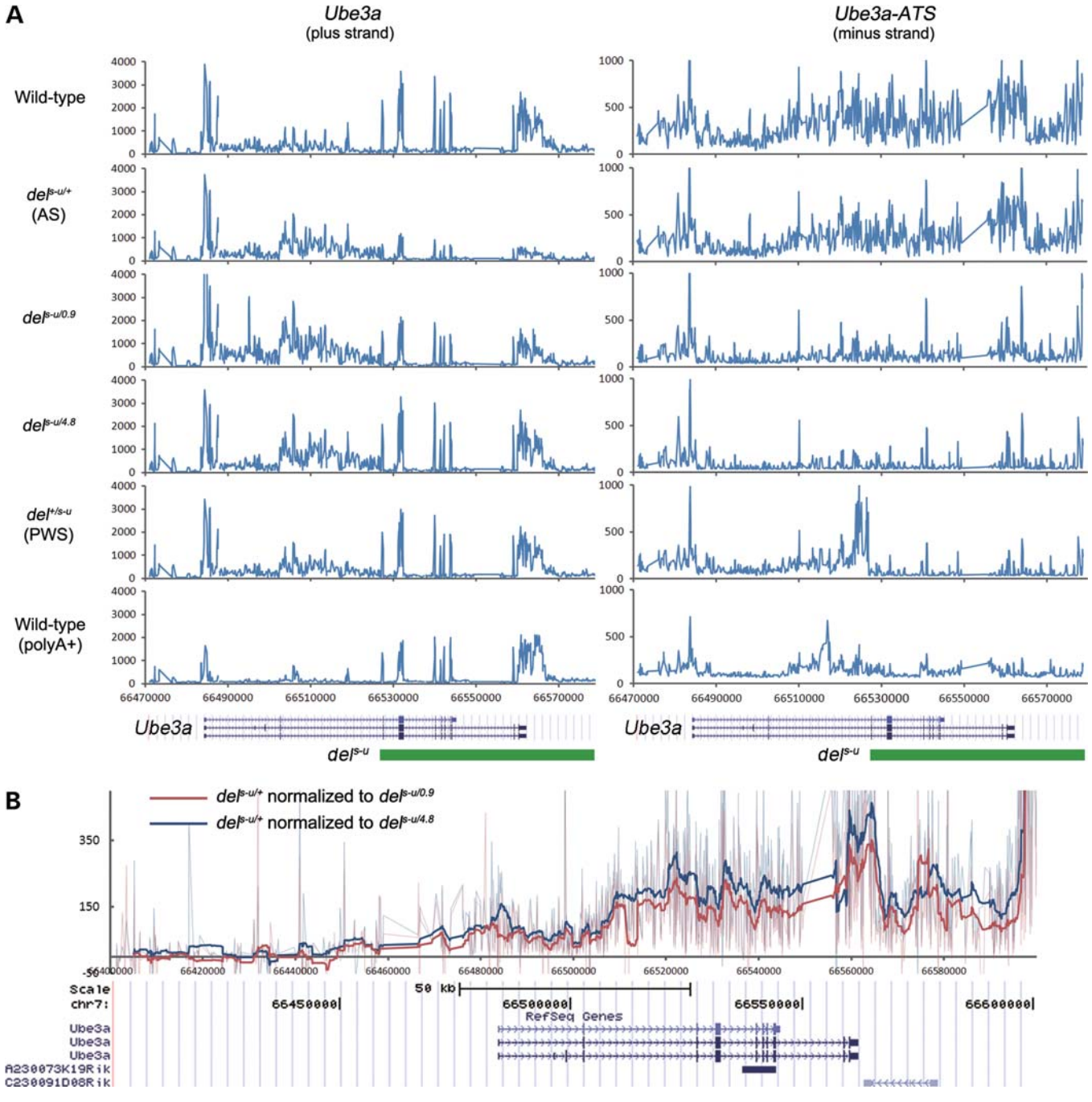

Figure 4. Differential expression of *Ube3a* and *Ube3a-ATS* is detected by the strand-specific microarray. (**A**) Total RNAs or polyA+ RNAs extracted from newborn mouse brains with various genotypes were reverse-transcribed, labeled and hybridized to the custom-designed strand-specific microarray. The microarray includes probes from both plus and minus strands of the *Ube3a* region, which hybridized to *Ube3a* and *Ube3a-ATS* cDNA, respectively. Normalized signal intensity (*y*-axis) was plotted against genomic coordinates (*x*-axis, NCBI37/mm9 build). The genomic segment deleted in $del^{s\text{-}u}$ is marked by the green bar. Noisy peaks to the left of the deletion boundary in some of the samples are probably artifacts arising from the ectopic expression of the selection marker inserted in the deletion region. (**B**) To reduce the background noise, the relative intensity of *Ube3a-ATS* was calculated as the difference between $del^{s\text{-}u/+}$ and $del^{s\text{-}u/0.9}$ or $del^{s\text{-}u/4.8}$. The light lines represent the relative intensity and the dark lines are the moving average of 20 probes.

Therapies for Angelman syndrome

Patients of Angelman syndrome suffer from developmental delay, speech impairment and seizures. Therapies for Angelman syndrome are limited and mainly focus on symptomatic management (8). In the present study, we showed that *Ube3a-ATS* functioned to suppress paternal *Ube3a* in mice and that the reduction in *Ube3a-ATS* expression by genetic manipulations was sufficient to activate paternal *Ube3a*. Given the conservation of the PWS/AS region between mouse and human, the activation of paternal *UBE3A* through inhibiting *UBE3A-ATS* expression/

transcription will be a promising strategy for the development of Angelman syndrome therapy.

Recently, topoisomerase inhibitors, currently used in cancer treatment, were found to unsilence paternal *Ube3a* expression very effectively in both neuronal culture system and mice (44). Although the exact mechanism of unsilencing remains unknown, evidence suggested that it may do so through reducing the expression of *Ube3a-ATS*. The effect of the drugs on the IC appears to be minimal, if there is any. This finding demonstrated nicely that targeting *Ube3a-ATS* can lead to therapies for Angelman syndrome.

Despite the promising and encouraging results of topoisomerase inhibitors, the non-specific nature of the drugs and their potential effect of inducing single- and double-strand breaks in cells may become an issue of safety in the future. Sequence-specific inhibition of *UBE3A-ATS* by oligonucleotide therapies has advantages over topoisomerase inhibitors in this point of view. Although it is unknown if transcription plays a role in repressing paternal *UBE3A*, using oligonucleotides to degrade already synthesized *UBE3A-ATS* might be more feasible to achieve than blocking transcription given the currently available technology. Chemically modified antisense oligonucleotides have better penetrance into the nucleus than siRNAs and degrade targeted molecules via RNase H cleavage. Efficient knockdown of a nuclear retained large ncRNA *Malat1* has been achieved in cell culture by this method (45). Large-scale screening of small oligonucleotides could be performed to identify molecules that are able to activate paternal *Ube3a* via the antisense RNA. Neuronal cultures derived from the $Ube3a^{+/YFP}$ mouse model could provide a good system for high-throughput screening, although a better model with a reporter linked to *Ube3a-ATS* may need to be further developed.

MATERIALS AND METHODS

Animals

Animals were housed under the standard conditions in a pathogen-free mouse facility. All procedures were performed in accordance with NIH guidelines and approved by the Baylor College of Medicine Institutional Animal Care and Use Committee (IACUC). Mice were sacrificed at P0-P3 for primary neuronal cultures, at P0 for brain RNA and protein extraction at P14 for bisulfite sequencing at 1–2 months old and for immunostaining.

Primary neuronal culture

Neuronal culture was performed as described previously (12). Specifically, chopped cortical hemispheres were digested with 0.25% trypsin and mechanically dissociated. Neurons were cultured in Neurobasal Medium (Invitrogen, Carlsbad, CA, USA) supplemented with B27 (Invitrogen) on plates coated with poly-D-lysine (Sigma, St Louis, MO, USA). Half of the medium was changed every 3 days.

RNA isolation and q-PCR

Total RNA was prepared with miRNeasy Mini Kit (Qiagen, Valencia, CA, USA). On-column DNase treatment was performed for all the samples. The mRNA was purified from 10 to 30 μg of total RNA with oligo(dT) beads supplied in Illumina mRNA-seq Sample Preparation Kit according to the manufacturer's instructions (Illumina, San Diego, CA, USA). The cDNA was then generated using 0.2–1 μg of total RNA with SuperScript III First-Strand Synthesis System (Invitrogen), and q-PCR was performed using Applied Biosystems StepOnePlus Real-Time PCR System and SYBR Green Master Mix (Applied Biosystems, Carlsbad, CA, USA). Primers used are listed in Supplementary Material, Table S1.

Bisulfite sequencing

F1 hybrids of C57BL/6 and CAST.chr7 were used in all bisulfite sequencing analysis in which SNPs were used to distinguish parental alleles. Genomic DNA (1 μg) was bisulfite-converted with EpiTect Bisulfite Kits (Qiagen) and 1 μl of converted DNA was used as the template for PCR with HotStarTaq DNA polymerase (Qiagen). The *Snrpn* intron1 region was amplified using primers *bis*-S-F (AATTTAGATATTTTTATTTTTGAGAA TTGG) or *bis*-0.9-S-F (TTAGGAAGTTTTGTTTTTAAAA TTAATAAT) and *bis*-S-R (CCCTATAACCCACTAACTA CATCAAC). The PCR product was separated on an agarose gel, extracted with MinElute Gel Extraction Kit (Qiagen) and cloned using TOPO TA Cloning Kit for Sequencing (Invitrogen). Inserts were then amplified with M13F and M13R primers from individual clones and sequenced.

Immunofluorescence staining

Mice of a specific genotype were anesthetized and perfused with 4% paraformaldehyde. Sagital sections of 5-μm thick were prepared from paraffin-embedded mouse brains. After gradient rehydration, antigen retrieval was done by incubating sections with boiling sodium citrate buffer (0.01 M, pH 6.0) for 15 min. Slides were permeabilized with 0.5% Triton X-100 in phosphate buffered saline (PBS) and blocked with 5% goat serum (Sigma) for 1 h each at room temperature. Sections were incubated with primary antibodies at 4°C overnight in a humid chamber with gentle agitation. Rabbit polyclonal anti-Ube3a (A300-352A, Bethyl Laboratories, Montgomery, TX, USA) was diluted 1:500 and mouse monoclonal anti-NeuN (MAB377, Millipore, Billerica, MA, USA) was diluted 1:500. After three washes in 0.5% Tween-20 in PBS, the secondary antibody of goat-anti-rabbit conjugated with Alexa Fluor 488 or goat-anti-mouse conjugated with Alexa Fluor 555 (Invitrogen, 1:1000 dilution) was applied to the slides for 1 h at room temperature. Immunostaining of cultured cells was performed similarly. Rabbit polyclonal anti-YFP (NB600-308, Novus Biologicals, Littleton, CO, USA) was diluted 1:2500 and mouse monoclonal anti-Map2 (MAB3418, Millipore) was diluted 1:1000. Images were taken using an LSM 510 Zeiss confocal microscope (Zeiss, Oberkochen, Germany). Z stack was performed when imaging cultured cells. Image processing and quantification of staining intensity was performed with ImageJ.

Western blot

Mouse brains or cell cultures were homogenized and lysed in RIPA buffer (0.75 M NaCl, 0.1% Triton X-100, 0.5% sodium

deoxycholate, 0.1% sodium dodecyl sulfate, 0.05 M Tris) containing cOmplete Protease Inhibitor Cocktail (Roche, Indianapolis, IN, USA). Protein extracts were separated on a 7.5% Mini-PROTEAN TGX Precast Gel (Bio-Rad Laboratories, Hercules, CA, USA), and western blot was performed as described previously (12). Mouse monoclonal anti-Ube3a was diluted at 1:500 (611416, BD Biosciences, Franklin Lakes, NJ, USA), and mouse monoclonal anti-β-tubulin was diluted at 1:20 000 (T9026, Sigma). Peroxidase-conjugated secondary anti-mouse was used at 1:1000 to 1:10 000 (Vector Labs, Burlingame, CA, USA).

Generation of the targeting vector and knock-in ES cell lines

EpA0 construct consisting of triple SV40 polyA sites as well as a splicing acceptor site and a loxP site (a gift from Dr Thomas Cooper, Baylor College of Medicine) (46) was cloned together with a PCR fragment of *loxP-FRT-Neo-FRT*. Recombineering was performed in BAC clone bMQ311i10 (Source BioScience, UK) utilizing a highly efficient protocol (47). Insertion of the *SV40-neo* cassette was designed to occur at chr7:66573289 (NCBI37/mm9). Left and right homologous arms are ∼5 kb both. Targeting vectors were electroporated into primary ES cell lines of $Ube3a^{+/YFP}$ generated from the cross of male $Ube3a^{+/YFP}$ with female WT. Recombinant clones were identified by Southern blot with *Bgl*II digestion and *cis* and *trans* clones were identified by Southern blot with *Sph*I digestion.

Neuronal differentiation of ES cells

Neuronal differentiation of ES cells was performed as reported previously (34) with some modifications. About 1.5×10^6 ES cells were collected and seeded in 10-ml N2/B27 medium [Dulbecco's modified Eagle medium (DMEM)/F12 supplemented with N2 and B27] mEB medium [Knockout DMEM with 10% fetal bovine serum (FBS), non-essential amino acids, L-glutamine and β-mercaptoethanol] onto non-adherent Petri dishes (Greiner Bio-one, Kaysville, UT, USA). The medium was changed every 2 days and 5 μM retinoic acid (Sigma) was added to the medium starting from day 4. On day 8, floating neural spheres were collected and trypsinized to single-cell suspension in N2 medium (DMEM/F12 supplemented with N2 and 1% FBS). About 1×10^6cells/well were seeded onto 6-well plates pretreated with 20 μg/ml poly-D-lysine (Sigma) and 5 μg/ml laminin (BD Bioscience) overnight or 2×10^5 cells/well onto 12 mm poly-D-lysine coated glass cover-slips (BD Bioscience). Two days later, the medium was changed to the N2/B27 medium (DMEM/F12 supplemented with N2 and B27) plus 1 μM Ara-C. The culture was harvested or fixed on day 14.

Strand-specific microarray and analysis

A custom-designed 8 × 60K comparative genomic hybridization (CGH) array was used for analysis (Agilent, Santa Clara, CA, USA). Agilent HD probes (plus-strand probes) were selected from genomic region chr7: 65 910 585–67 600 789 (mouse genome assembly NCBI37/mm9, covering *Snrpn* upstream exons to *Atp10a*) using Agilent eArray online software. Probes from four selected control genes *Gapdh*, *Pgk1*, *Tfrc* and *Actb* were also included. Reverse-complement probes were then manually generated as minus-strand probes. Total mouse cerebral cortical RNA (15 μg) or 750 ng polyA+ RNA supplemented with *E. coli* rRNA (Roche) was converted to Cy5-labeled first-strand cDNA by ChipShot Labeling System according to the manufacturer's instructions (Promega, Madison, WI, USA). Labeled cDNA was purified using BioPrime Array CGH Genomic Labeling System (Invitrogen). The labeled cDNA (1 μg) was hybridized to the microarray with Agilent Oligo aCGH Hybridization Kit at 65°C overnight. The slides were washed according to the Agilent aCGH protocol and scanned into image files using Agilent G2505C Microarray Scanner. The data were processed with Agilent Feature Extraction software (v10.9) using protocol GE2-NonAT_107_Sep09. Further data processing was performed using Microsoft Excel. Detailed information and the entire data set can be accessed under GEO accession number GSE29254.

SUPPLEMENTARY MATERIAL

Supplementary Material is available at *HMG* online.

ACKNOWLEDGEMENTS

We thank Isabel Lorenzo and the Mouse ES Cell Core Facility of Baylor College of Medicine for the help in generating primary mouse ES cell lines and in electroporation. We thank Dr Thomas Cooper for generously offering EpA0 construct and Dr Nicholas J. Justice for offering reagents of recombineering. We thank Dr Hui Zheng and her lab people for extremely valuable technical assistance and generous sharing of reagents and equipment. We thank Dr Richard C. Atkinson and Baylor College of Medicine IDDRC confocal microscopy core for the assistance.

Conflict of Interest statement. None declared.

FUNDING

This work was supported by National Institution of Health (R01 HD037283).

REFERENCES

1. Edwards, C.A. and Ferguson-Smith, A.C. (2007) Mechanisms regulating imprinted genes in clusters. *Curr. Opin. Cell Biol.*, **19**, 281–289.
2. Horsthemke, B. (2010) Mechanisms of imprint dysregulation. *Am. J. Med. Genet. C Semin. Med. Genet.*, **154C**, 321–328.
3. Buiting, K. (2010) Prader-Willi syndrome and Angelman syndrome. *Am. J. Med. Genet. C Semin. Med. Genet.*, **154C**, 365–376.
4. Horsthemke, B. and Wagstaff, J. (2008) Mechanisms of imprinting of the Prader-Willi/Angelman region. *Am. J. Med. Genet. A*, **146A**, 2041–2052.
5. Kantor, B., Makedonski, K., Green-Finberg, Y., Shemer, R. and Razin, A. (2004) Control elements within the PWS/AS imprinting box and their function in the imprinting process. *Hum. Mol. Genet.*, **13**, 751–762.
6. Chamberlain, S.J. and Lalande, M. (2010) Angelman syndrome, a genomic imprinting disorder of the brain. *J. Neurosci.*, **30**, 9958–9963.
7. Van Buggenhout, G. and Fryns, J.P. (2009) Angelman syndrome (AS, MIM 105830). *Eur. J. Hum. Genet.*, **17**, 1367–1373.
8. Williams, C.A., Driscoll, D.J. and Dagli, A.I. (2010) Clinical and genetic aspects of Angelman syndrome. *Genet. Med.*, **12**, 385–395.

9. Rougeulle, C., Glatt, H. and Lalande, M. (1997) The Angelman syndrome candidate gene, UBE3A/E6-AP, is imprinted in brain. *Nat. Genet.*, **17**, 14–15.
10. Vu, T.H. and Hoffman, A.R. (1997) Imprinting of the Angelman syndrome gene, UBE3A, is restricted to brain. *Nat. Genet.*, **17**, 12–13.
11. Yamasaki, K., Joh, K., Ohta, T., Masuzaki, H., Ishimaru, T., Mukai, T., Niikawa, N., Ogawa, M., Wagstaff, J. and Kishino, T. (2003) Neurons but not glial cells show reciprocal imprinting of sense and antisense transcripts of Ube3a. *Hum. Mol. Genet.*, **12**, 837–847.
12. Dindot, S.V., Antalffy, B.A., Bhattacharjee, M.B. and Beaudet, A.L. (2008) The Angelman syndrome ubiquitin ligase localizes to the synapse and nucleus, and maternal deficiency results in abnormal dendritic spine morphology. *Hum. Mol. Genet.*, **17**, 111–118.
13. Lossie, A.C., Whitney, M.M., Amidon, D., Dong, H.J., Chen, P., Theriaque, D., Hutson, A., Nicholls, R.D., Zori, R.T., Williams, C.A. *et al.* (2001) Distinct phenotypes distinguish the molecular classes of Angelman syndrome. *J. Med. Genet.*, **38**, 834–845.
14. Makedonski, K., Abuhatzira, L., Kaufman, Y., Razin, A. and Shemer, R. (2005) MeCP2 deficiency in Rett syndrome causes epigenetic aberrations at the PWS/AS imprinting center that affects UBE3A expression. *Hum. Mol. Genet.*, **14**, 1049–1058.
15. Jiang, Y.H., Sahoo, T., Michaelis, R.C., Bercovich, D., Bressler, J., Kashork, C.D., Liu, Q., Shaffer, L.G., Schroer, R.J., Stockton, D.W. *et al.* (2004) A mixed epigenetic/genetic model for oligogenic inheritance of autism with a limited role for UBE3A. *Am. J. Med. Genet. A*, **131**, 1–10.
16. Latos, P.A. and Barlow, D.P. (2009) Regulation of imprinted expression by macro non-coding RNAs. *RNA Biol.*, **6**, 100–106.
17. Mohammad, F., Mondal, T. and Kanduri, C. (2009) Epigenetics of imprinted long noncoding RNAs. *Epigenetics*, **4**, 277–286.
18. Pauler, F.M., Koerner, M.V. and Barlow, D.P. (2007) Silencing by imprinted noncoding RNAs: is transcription the answer? *Trends Genet*, **23**, 284–292.
19. Sleutels, F., Zwart, R. and Barlow, D.P. (2002) The non-coding Air RNA is required for silencing autosomal imprinted genes. *Nature*, **415**, 810–813.
20. Mancini-Dinardo, D., Steele, S.J., Levorse, J.M., Ingram, R.S. and Tilghman, S.M. (2006) Elongation of the Kcnq1ot1 transcript is required for genomic imprinting of neighboring genes. *Genes Dev.*, **20**, 1268–1282.
21. Seidl, C.I., Stricker, S.H. and Barlow, D.P. (2006) The imprinted Air ncRNA is an atypical RNAPII transcript that evades splicing and escapes nuclear export. *EMBO J.*, **25**, 3565–3575.
22. Pandey, R.R., Mondal, T., Mohammad, F., Enroth, S., Redrup, L., Komorowski, J., Nagano, T., Mancini-Dinardo, D. and Kanduri, C. (2008) Kcnq1ot1 antisense noncoding RNA mediates lineage-specific transcriptional silencing through chromatin-level regulation. *Mol. Cell*, **32**, 232–246.
23. Rougeulle, C., Cardoso, C., Fontes, M., Colleaux, L. and Lalande, M. (1998) An imprinted antisense RNA overlaps UBE3A and a second maternally expressed transcript. *Nat. Genet.*, **19**, 15–16.
24. Runte, M., Huttenhofer, A., Gross, S., Kiefmann, M., Horsthemke, B. and Buiting, K. (2001) The IC-SNURF-SNRPN transcript serves as a host for multiple small nucleolar RNA species and as an antisense RNA for UBE3A. *Hum. Mol. Genet.*, **10**, 2687–2700.
25. Landers, M., Bancescu, D.L., Le Meur, E., Rougeulle, C., Glatt-Deeley, H., Brannan, C., Muscatelli, F. and Lalande, M. (2004) Regulation of the large (approximately 1000 kb) imprinted murine Ube3a antisense transcript by alternative exons upstream of Snurf/Snrpn. *Nucleic Acids Res.*, **32**, 3480–3492.
26. Le Meur, E., Watrin, F., Landers, M., Sturny, R., Lalande, M. and Muscatelli, F. (2005) Dynamic developmental regulation of the large non-coding RNA associated with the mouse 7C imprinted chromosomal region. *Dev. Biol.*, **286**, 587–600.
27. Chamberlain, S.J. and Brannan, C.I. (2001) The Prader-Willi syndrome imprinting center activates the paternally expressed murine Ube3a antisense transcript but represses paternal Ube3a. *Genomics*, **73**, 316–322.
28. Johnstone, K.A., DuBose, A.J., Futtner, C.R., Elmore, M.D., Brannan, C.I. and Resnick, J.L. (2006) A human imprinting centre demonstrates conserved acquisition but diverged maintenance of imprinting in a mouse model for Angelman syndrome imprinting defects. *Hum. Mol. Genet.*, **15**, 393–404.
29. Lalande, M. and Calciano, M.A. (2007) Molecular epigenetics of Angelman syndrome. *Cell. Mol. Life Sci.*, **64**, 947–960.
30. Landers, M., Calciano, M.A., Colosi, D., Glatt-Deeley, H., Wagstaff, J. and Lalande, M. (2005) Maternal disruption of Ube3a leads to increased expression of Ube3a-ATS in trans. *Nucleic Acids Res.*, **33**, 3976–3984.
31. Bressler, J., Tsai, T.F., Wu, M.Y., Tsai, S.F., Ramirez, M.A., Armstrong, D. and Beaudet, A.L. (2001) The SNRPN promoter is not required for genomic imprinting of the Prader-Willi/Angelman domain in mice. *Nat. Genet.*, **28**, 232–240.
32. Wakeland, E., Morel, L., Achey, K., Yui, M. and Longmate, J. (1997) Speed congenics: a classic technique in the fast lane (relatively speaking). *Immunol. Today*, **18**, 472–477.
33. Tsai, T.F., Jiang, Y.H., Bressler, J., Armstrong, D. and Beaudet, A.L. (1999) Paternal deletion from Snrpn to Ube3a in the mouse causes hypotonia, growth retardation and partial lethality and provides evidence for a gene contributing to Prader-Willi syndrome. *Hum. Mol. Genet.*, **8**, 1357–1364.
34. Bibel, M., Richter, J., Schrenk, K., Tucker, K.L., Staiger, V., Korte, M., Goetz, M. and Barde, Y.A. (2004) Differentiation of mouse embryonic stem cells into a defined neuronal lineage. *Nat. Neurosci.*, **7**, 1003–1009.
35. Numata, K., Kohama, C., Abe, K. and Kiyosawa, H. (2011) Highly parallel SNP genotyping reveals high-resolution landscape of mono-allelic Ube3a expression associated with locus-wide antisense transcription. *Nucleic Acids Res.*, **39**, 2649–2657.
36. Shibata, S. and Lee, J.T. (2004) Tsix transcription- versus RNA-based mechanisms in Xist repression and epigenetic choice. *Curr. Biol.*, **14**, 1747–1754.
37. Jiang, Y., Lev-Lehman, E., Bressler, J., Tsai, T.F. and Beaudet, A.L. (1999) Genetics of Angelman syndrome. *Am. J. Hum. Genet.*, **65**, 1–6.
38. Lyle, R., Watanabe, D., te Vruchte, D., Lerchner, W., Smrzka, O.W., Wutz, A., Schageman, J., Hahner, L., Davies, C. and Barlow, D.P. (2000) The imprinted antisense RNA at the Igf2r locus overlaps but does not imprint Mas1. *Nat. Genet.*, **25**, 19–21.
39. Santoro, F. and Barlow, D.P. (2011) Developmental control of imprinted expression by macro non-coding RNAs. *Semin. Cell Dev. Biol.*, **22**, 328–335.
40. Herzing, L.B., Kim, S.J., Cook, E.H. Jr. and Ledbetter, D.H. (2001) The human aminophospholipid-transporting ATPase gene ATP10C maps adjacent to UBE3A and exhibits similar imprinted expression. *Am. J. Hum. Genet.*, **68**, 1501–1505.
41. Meguro, M., Kashiwagi, A., Mitsuya, K., Nakao, M., Kondo, I., Saitoh, S. and Oshimura, M. (2001) A novel maternally expressed gene, ATP10C, encodes a putative aminophospholipid translocase associated with Angelman syndrome. *Nat. Genet.*, **28**, 19–20.
42. Jiang, Y.H., Pan, Y., Zhu, L., Landa, L., Yoo, J., Spencer, C., Lorenzo, I., Brilliant, M., Noebels, J. and Beaudet, A.L. (2010) Altered ultrasonic vocalization and impaired learning and memory in Angelman syndrome mouse model with a large maternal deletion from Ube3a to Gabrb3. *PLoS One*, **5**, e12278.
43. DuBose, A.J., Johnstone, K.A., Smith, E.Y., Hallett, R.A. and Resnick, J.L. (2010) Atp10a, a gene adjacent to the PWS/AS gene cluster, is not imprinted in mouse and is insensitive to the PWS-IC. *Neurogenetics*, **11**, 145–151.
44. Huang, H.S., Allen, J.A., Mabb, A.M., King, I.F., Miriyala, J., Taylor-Blake, B., Sciaky, N., Dutton, J.W. Jr, Lee, H.M., Chen, X. *et al.* (2012) Topoisomerase inhibitors unsilence the dormant allele of Ube3a in neurons. *Nature*, **481**, 185–189.
45. Bernard, D., Prasanth, K.V., Tripathi, V., Colasse, S., Nakamura, T., Xuan, Z., Zhang, M.Q., Sedel, F., Jourdren, L., Coulpier, F. *et al.* (2010) A long nuclear-retained non-coding RNA regulates synaptogenesis by modulating gene expression. *EMBO J.*, **29**, 3082–3093.
46. Wang, G.S., Kearney, D.L., De Biasi, M., Taffet, G. and Cooper, T.A. (2007) Elevation of RNA-binding protein CUGBP1 is an early event in an inducible heart-specific mouse model of myotonic dystrophy. *J. Clin. Invest.*, **117**, 2802–2811.
47. Chan, W., Costantino, N., Li, R., Lee, S.C., Su, Q., Melvin, D., Court, D.L. and Liu, P. (2007) A recombineering based approach for high-throughput conditional knockout targeting vector construction. *Nucleic Acids Res.*, **35**, e64.
48. Redrup, L., Branco, M.R., Perdeaux, E.R., Krueger, C., Lewis, A., Santos, F., Nagano, T., Cobb, B.S., Fraser, P. and Reik, W. (2009) The long noncoding RNA Kcnq1ot1 organises a lineage-specific nuclear domain for epigenetic gene silencing. *Development*, **136**, 525–530.